Arterial Spin Labeled Perfusion MRI

John A. Detre, M.D.

Center for Functional Neuroimaging, Department of Neurology and Radiology, University of Pennsylvania, Philadelphia, PA, USA

Perfusion refers to the delivery of oxygen and nutrients to tissues by means of blood flow and is one of the most fundamental physiological parameters. Disorders of perfusion also account for most of the leading causes of medical disability and mortality. While measurements of perfusion are of direct diagnostic value in vascular disorders, perfusion measurements also serve as biomarkers for a broader range of physiological and pathophysiological functions. A close coupling between cerebral blood flow and metabolism allows regional brain function to be assessed through measurements of cerebral perfusion and increased vascularity of neoplasms allows tumor perfusion to be used as a measure of tumor grade and to monitor the response to tumor therapy.

Classical tissue perfusion is measured using a diffusible tracer that can exchange between the vascular compartment and tissue. This yields a perfusion measurement in units of milliliters of blood flow per gram of tissue per unit time (ml/g/min). However, owing to the relative ease of inferring hemodynamic function from the passage of an intravascular tracer, the term "perfusion imaging" has also been applied to measurements of perfusion-related parameters such as mean transit time and blood volume that can be related to perfusion through the Central Volume Principle. In the field of MRI, most people associate the concept of perfusion imaging with dynamic susceptibility contrast imaging using a relaxation contrast agent. However, there are also several methods for the measurement of classical tissue perfusion using MRI. Diffusible tracers that can be monitored with MRI include fluorinated halocarbons [1], deuterated water ($^{2}H2O$) [2, 3], ^{17}O-water [4], and potentially ^{13}C labeled hydrocarbons.

Magnetically labeled endogenous blood water can also be used as a tracer for perfusion MRI. To accomplish this, the longitudinal magnetization of arterial blood water must be manipulated so that it differs from the tissue magnetization. It is quite analogous to the use of 15O-water for PET perfusion imaging except that the magnetic tracer decays with T1 instead of a radioactive decay and the ASL

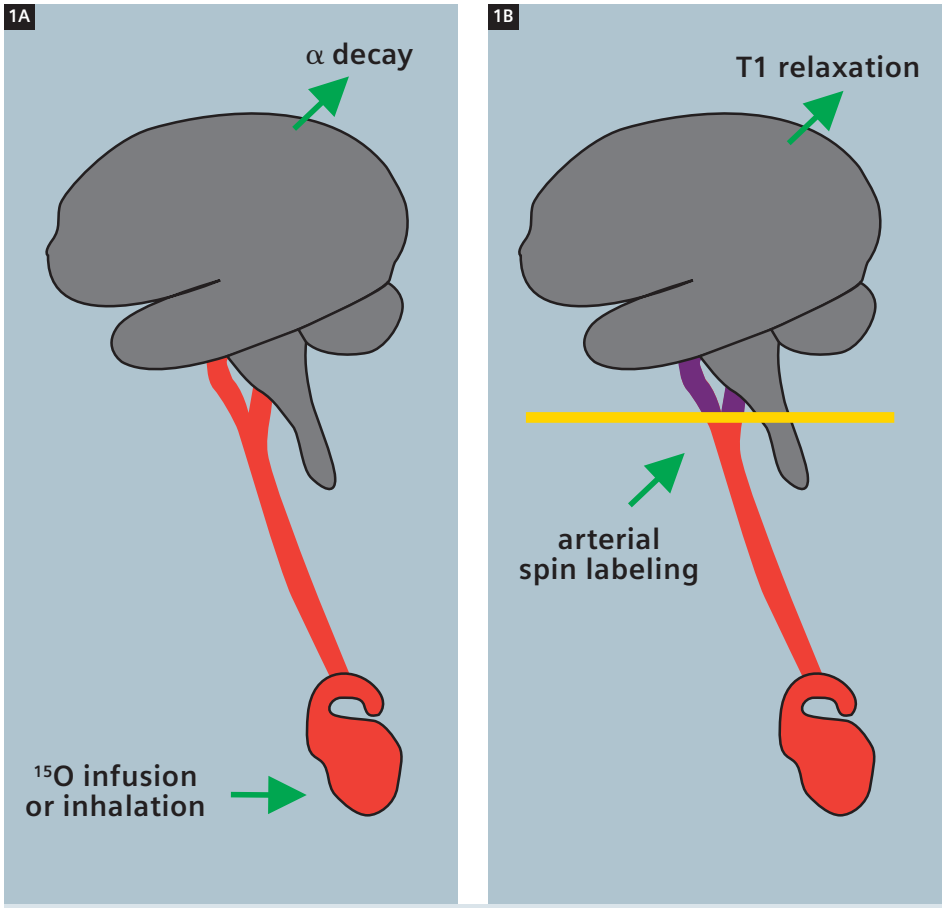

1 Concept of Arterial Spin Labeling (ASL), comparing 15O-PET (Fig. 1A)) and ASL (Fig. 1B) approaches. In ASL, endogenous arterial blood water is magnetically labeled instead of exogenously administered tracer, and the magnetic label decays with T1 instead of radioactive decay (α).

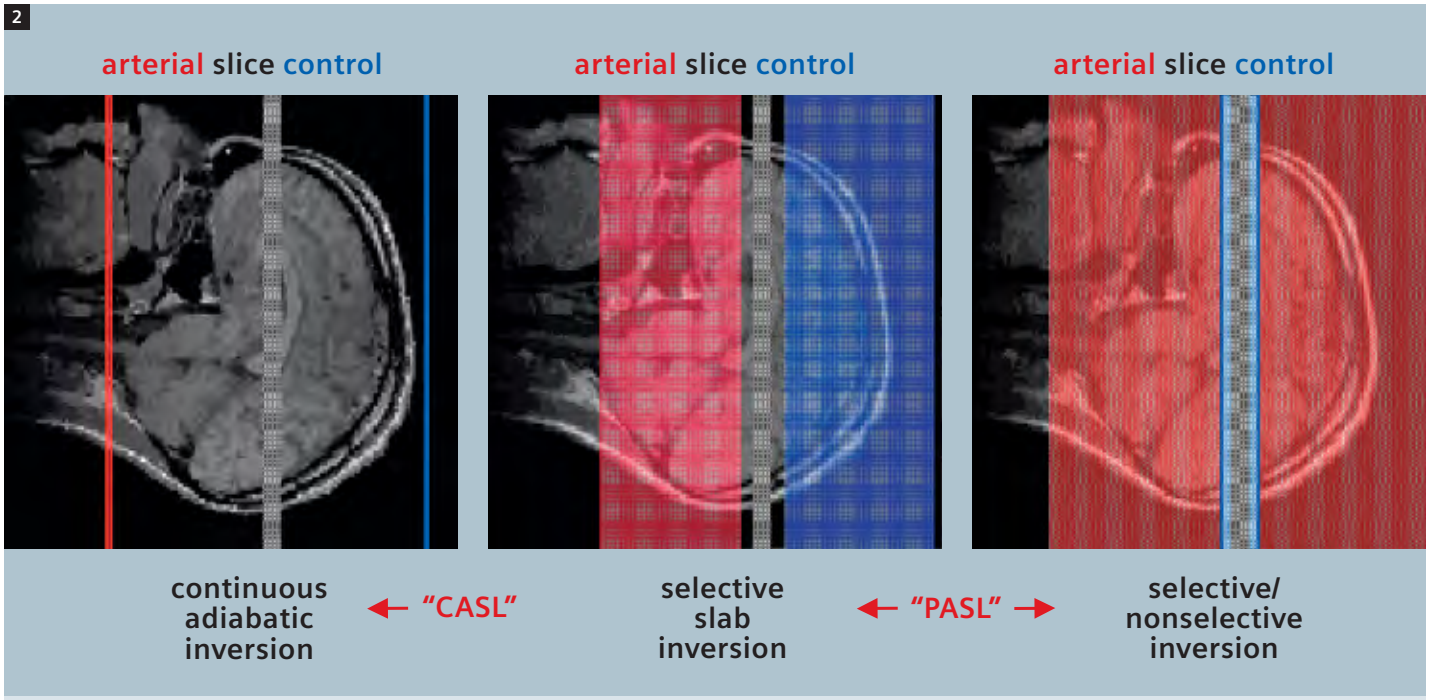

2 Schematic diagram illustrating arterial spin labeling strategies. Continuous ASL (CASL, left) labels arterial spins as they flow through a labeling plane. Pulsed ASL (PASL, middle and right) labels arterial spins using a spatially selective labeling pulse. Applications to single-slice imaging are illustrated for simplicity. Somewhat more complex schemes are used for multislice imaging.

approach is completely noninvasive. Because T1 relaxation is approximately 100 times faster than the radioactive decay rate of 15O, only a small amount of labeled water accumulates, though the temporal resolution is also correspondingly higher. The subtle difference between images acquired with and without arterial spin labeling (ASL) can be modeled to derive a calculated blood flow image showing perfusion in ml/g/min at each voxel. Key parameters required for ASL quantification include knowledge or assumptions about the T1 values in blood and tissue, the labeling efficiency, and the arterial transit time [5, 6]. ASL can be combined with any imaging sequence and theoretically provides a flow image that is completely independent of scanning parameters; As such, it represents one of the few MRI contrast mechanisms for which the physiological basis is really well understood. In practice, most ASL measurements are made with some compromises trading off sensitivity and convenience for a less pure measurement of tissue blood flow.

Arterial spin labeling can be accomplished using a variety of approaches and in nearly any organ. Most ASL has been carried out in the brain because the arterial supply is extremely well defined and perfusion to brain tissue is high. However, ASL studies have also successfully been carried out in kidney, lung, retina, heart, and skeletal muscle. The most common ASL approaches use either pulsed labeling (PASL) with an instantaneous spatially selective saturation or inversion pulse [7], or continuous labeling (CASL), most typically by flow driven adiabatic fast passage [8]. In some PASL methods, a spatially selective inversion pulse is administered to the tissue rather than to arterial blood [9]. More recently there have also been efforts label based on velocity rather than spatial selectivity for tissue arterial supply [10]. The first publication on ASL perfusion MRI actually used pseudocontinuous saturation to dephase arterial blood water in the neck of a rat [11]. Prior to that time, the idea of labeling arterial blood water had been considered primarily as a means for visualizing intraluminal flow in arteries and veins [12, 13]. Continuous labeling schemes allow brain magnetization to reach a steady-state that maximizes the signal difference between labeled and unlabeled conditions [14], though this occurs at the expense of both increased SAR deposition and magnetization transfer effects that complicate both the accurate measurement of the control (unlabeled) condition, and the extension to multislice imaging. Some groups have addressed this using a separate labeling coil [15], while others have pursued single coil approaches [16]. The myriad technical details of ASL implementation are beyond the scope of this article, but key advances have focused on improved labeling, improved measurements of the subtle effects of ASL on tissue signal, and improved modeling of measured signal changes in terms of tissue blood flow. For CBF, current tech-

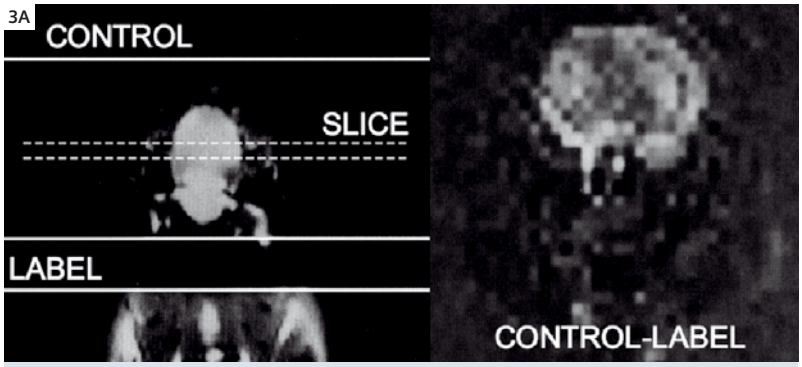

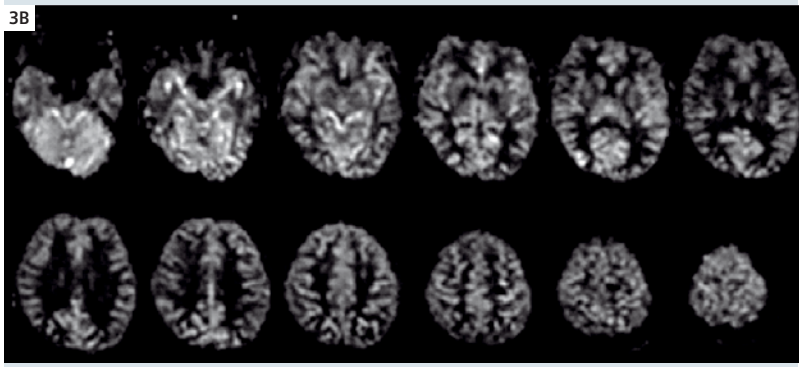

3 The original demonstration of ASL using pseudocontinuous ASL in the rat brain [11]. **(Fig. 3A)**
Multislice PASL of human brain acquired from a normal volunteer at 3T [18]. **(Fig. 3B)**

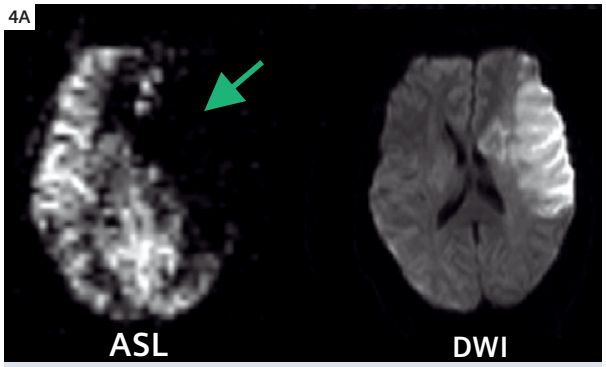

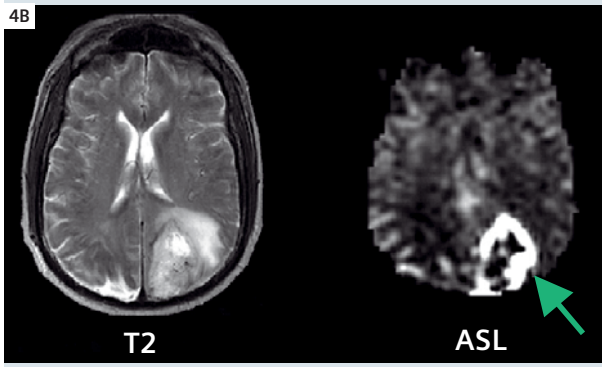

4 Representative clinical applications of ASL showing hypoperfusion in an acute stroke **(Fig. 4A)** and hyperperfusion in a glioblastoma **(Fig. 4B)**. For more details on clinical applications of ASL see [31].

nology provides a reasonably good whole-brain image in just a few minutes of scanning. ASL methods particularly benefit from high magnetic field trengths because not only is the sensitivity higher, but T1 also lengthens, allowing more label to accumulate [17, 18]. ASL methods also benefit from the increased sensitivity provided by multicoil receivers and are minimally degraded by parallel imaging [19]. The use of a body transmitter benefits PASL by allowing a larger region for arterial inversion but necessitates a more elaborate approach for CASL, termed pseudo-continuous labeling [20].

In clinical neuroscience, while the application of ASL perfusion MRI to the diagnosis and management of acute stroke is both obvious and feasible, the clinical utility of ASL is likely much broader since only a minority of acute stroke patients undergo MRI. ASL perfusion MRI could greatly enhance the evaluation of both TIA (Transient Ischemic Attack) and chronic cerebrovascular disease by quantifying regional CBF in specific vascular territories where interventions may be planned, or by allowing the effects of pharmacological therapies on CBF to be evaluated. Several approaches now also exist for selective arterial labeling, allowing the perfusion distribution of specific arteries to be assessed independently [21, 22]. A challenge in the application of ASL to cerebrovascular disorders is that sensitivity decreases in regions with very low CBF and the presence of prolonged arterial transit times that can create regions of apparent hyperperfusion when labeled spins remain in large vessels due to prolonged arterial transit times. This artifact is usually easy to recognize and can be verified by the addition of spoiler gradients that dephase coherently flowing spins. Arterial transit times can even be quantified by comparing ASL images with and without spoiler gradients [23], providing access to a novel physiological parameter that likely reflects the recruitment collateral flow sources. Another significant application of ASL is in degenerative diseases, where specific patterns of hypoperfusion may be used to aid in differential diagnosis of disorders such as Alzheimer's disease [24] and frontotemporal dementia [25]. Finally, as noted above, perfusion of brain tumors typically correlates with their grade and potentially their response to therapies [26]. Undoubtedly, the clinical availability of noninvasive and quantitative CBF imaging will lead to numerous additional applications as further experience with this modality develops.

In basic neuroscience, ASL perfusion MRI can be used to localize task activation in a manner similar to BOLD fMRI (Blood Oxygen Level Dependent functional MR Imaging). Indeed, ASL based contrast derived from inversion recovery imaging of task activation was included in one of the earliest reports of fMRI in human brain [28]. Although relative CBF can be inferred from ASL images acquired without control labeling, acquisition of both labeled and control pairs are required for quantification of CBF. While this reduces the temporal resolution of ASL perfusion fMRI as compared to BOLD fMRI, it also

dramatically changes the noise properties of the data, providing sensitivity over much longer timescales [29]. ASL perfusion fMRI can also be used as a measure of brain function at rest, independent of any sensorimotor or cognitive task, and reveals regional changes in brain function associated with development [30], behavioral states [31], or genetic traits [32]. Because ASL measures a purely biological parameter, it should also be particularly valuable for multisite studies examining brain function on a variety of scanner platforms or longitudinally.

A limitation in the widespread use and dissemination of ASL perfusion MRI has been the absence of product sequences provided by vendors. The recent development of an ASL product by Siemens should help alleviate this limitation, at least for Siemens users. Other vendors will hopefully follow suit. The Siemens ASL product provides a robust PASL sequence with echoplanar readout and online calculation of CBF maps from the acquired data. Many of us involved in the early development and validation of ASL perfusion MRI are eager to see it translated to routine clinical use.

Dr. Detre is an inventor of ASL technology and has received royalties from the University of Pennsylvania for its licensure.

References

1 Eleff, S.M., M.D. Schnall, L. Ligetti, M. Osbakken, V.H. Subramanian, B. Chance and J.S.J. Leigh, Concurrent measurement of cerebral blood flow, sodium, lactate, and high-energy phosphate metabolism using 19F, 23Na, 1H, and 31P nuclear magnetic resonance spectroscopy. Magn. Reson. Med., 1988. 7: p. 412-24.

2 Ackerman, J.J., C.S. Ewy, N.N. Becker and R.A. Shalwitz, Deuterium nuclear magnetic resonance measurements of blood flow and tissue perfusion employing 2H2O as a freely diffusible tracer. Proc Natl Acad Sci U S A, 1987. 84(12): p. 4099-102.

3 Detre, J.A., V.H. Subramanian, M.D. Mitchell, D.S. Smith, A. Kobayashi, A. Zaman and J.S. Leigh, Measurement of regional cerebral blood flow in cat brain using intracarotid 2H2O and 2H NMR imaging. Magn. Reson. Med., 1990. 14: p. 389-395.

4 Pekar, J., L. Ligeti, Z. Ruttner, R.C. Lyon, T.M. Sinnwell, P. van Gelderen, D. Fiat, C.T. Moonen and A.C. McLaughlin, In vivo measurement of cerebral oxygen consumption and blood flow using 17O magnetic resonance imaging. Magn Reson Med, 1991. 21(2): p. 313-9.

5 Alsop, D.C. and J.A. Detre, Reduced transit-time sensitivity in noninvasive magnetic resonance imaging of human cerebral blood flow. J. Cereb. Blood Flow Metab., 1996. 16: p. 1236-1249.

6 Buxton, R.B., L.R. Frank, E.C. Wong, B. Siewert, S. Warach and R.R. Edelman, A general kinetic model for quantitative perfusion imaging with arterial spin labeling. Magn Reson Med, 1998. 40(3): p. 383-96.

7 Wong, E.C., R.B. Buxton and L.R. Frank, Implementation of quantitative perfusion imaging techniques for functional brain mapping using pulsed arterial spin labeling. NMR Biomed, 1997. 10(4-5): p. 237-49.

8 Williams, D.S., J.A. Detre, J.S. Leigh and A.P. Koretsky, Magnetic resonance imaging of perfusion using spin inversion of arterial water. Proc. Natl. Acad. Sci. USA, 1992. 89: p. 212-216.

9 Kim, S.G., Quantification of relative cerebral blood flow change by flow-sensitive alternating inversion recovery (FAIR) technique: application to functional mapping. Magn. Reson. Med., 1995. 34: p. 293-301.

10 Wong, E.C., M. Cronin, W.C. Wu, B. Inglis, L.R. Frank and T.T. Liu, Velocity-selective arterial spin labeling. Magn Reson Med, 2006. 55(6): p. 1334-41.

11 Detre, J.A., J.S. Leigh, D.S. Williams and A.P. Koretsky, Perfusion imaging. Magn. Reson. Med., 1992. 23: p. 37-45.

12 Sardashti, M., D.G. Schwartzberg, G.P. Stomp and W.T. Dixon, Spin labeling angiography of the carotids by presaturation and simplified adiabatic inversion. Magn. Reson. Med., 1990. 15: p. 192-200.

13 Singer, J.R. and L.E. Crooks, Nuclear magnetic resonance blood flow measurements in the human brain. Science, 1983. 221(4611): p. 654-6.

14 Wong, E.C., R.B. Buxton and L.R. Frank, A theoretical and experimental comparison of continuous and pulsed arterial spin labeling techniques for quantitative perfusion imaging. Magn Reson Med, 1998. 40(3): p. 348-55.

15 Zaharchuk, G., P.J. Ledden, K.K. Kwong, T.G. Reese, B.R. Rosen and L.L. Wald, Multislice perfusion and perfusion territory imaging in humans with separate label and image coils. Magn. Reson. Med., 1999. 41: p. 1093-8.

16 Alsop, D.C. and J.A. Detre, Multisection cerebral blood flow MR imaging with continuous arterial spin labeling. Radiology, 1998. 208: p. 410-16.

17 Wang, J., D.C. Alsop, L. Li, J. Listerud, J.B. Gonzalez-At, M.D. Schnall and J.A. Detre, Comparison of quantitative perfusion imaging using arterial spin labeling at 1.5 and 4.0 Tesla. Magn Reson Med, 2002. 48(2): p. 242-54.

18 Wang, J., Y. Zhang, R.L. Wolf, A.C. Roc, D.C. Alsop and J.A. Detre, Amplitude-modulated Continuous Arterial Spin-labeling 3.0-T Perfusion MR Imaging with a Single Coil: Feasibility Study. Radiology, 2005. 235: p. 218-28.

19 Wang, Z., J. Wang, T.J. Connick, G.S. Wetmore and J.A. Detre, Continuous ASL perfusion MRI with an array coil and parallel imaging at 3T. Magn Reson Med, 2005. 54(3): p. 732-7.

20 Garcia, D.M., C. de Bazelaire and D. Alsop, Pseudo-continuous Flow Driven Adiabatic Inversion for Arterial Spin Labeling. ISMRM 13th Scientific Meeting Proceedings, 2005: p. 37.

21 Hendrikse, J., J. van der Grond, H. Lu, P.C. van Zijl and X. Golay, Flow territory mapping of the cerebral arteries with regional perfusion MRI. Stroke, 2004. 35(4): p. 882-7.

22 Werner, R., K. Alfke, T. Schaeffter, A. Nabavi, H.M. Mehdorn and O. Jansen, Brain perfusion territory imaging applying oblique-plane arterial spin labeling with a standard send/receive head coil. Magn Reson Med, 2004. 52(6): p. 1443-7.

23 Wang, J., D.C. Alsop, H.K. Song, J.A. Maldjian, K. Tang, A.E. Salvucci and J.A. Detre, Arterial transit time imaging with flow encoding arterial spin tagging (FEAST). Magn Reson Med, 2003. 50(3): p. 599-607.

24 Alsop, D.C., J.A. Detre and M. Grossman, Assessment of cerebral blood flow in Alzheimer's disease by spin-labeled magnetic resonance imaging. Ann Neurol, 2000. 47(1): p. 93-100.

25 Du, A.T., G.H. Jahng, S. Hayasaka, J.H. Kramer, H.J. Rosen, M.L. Gorno-Tempini, K.P. Rankin, B.L. Miller, M.W. Weiner and N. Schuff, Hypoperfusion in frontotemporal dementia and Alzheimer disease by arterial spin labeling MRI. Neurology, 2006. 67(7): p. 1215-20.

26 Wolf, R.L., J. Wang, S. Wang, E.R. Melhem, M. O'Rourke D, K.D. Judy and J.A. Detre, Grading of CNS neoplasms using continuous arterial spin labeled perfusion MR imaging at 3 Tesla. J Magn Reson Imaging, 2005. 22(4): p. 475-482.

27 Wolf, R.L. and J.A. Detre, Clinical neuroimaging using arterial spin-labeled perfusion magnetic resonance imaging. Neurotherapeutics, 2007. 4(3): p. 346-59.

28 Kwong, K.K., J.W. Belliveau, D.A. Chesler, I.E. Goldberg, R.M. Weisskoff, B.P. Poncelet, D.N. Kennedy, B.E. Hoppel, M.S. Cohen and R. Turner, Dynamic magnetic resonance imaging of human brain activity during primary sensory stimulation. Proc. Natl. Acad. Sci. USA, 1992. 89: p. 5675-5679.

29 Aguirre, G.K., J.A. Detre and D.C. Alsop, Experimental design and the relative sensitivity of BOLD and perfusion fMRI. Neuroimage, 2002. 15: p. 488-500.

30 Wang, Z., M. Fernandez-Seara, D.C. Alsop, W.C. Liu, J.F. Flax, A.A. Benasich and J.A. Detre, Assessment of functional development in normal infant brain using arterial spin labeled perfusion MRI. Neuroimage, 2008. 39(3): p. 973-8.

31 Wang, J., H. Rao, G.S. Wetmore, P.M. Furlan, M. Korczykowski, D.F. Dinges and J.A. Detre, Perfusion functional MRI reveals cerebral blood flow pattern under psychological stress. Proc Natl Acad Sci U S A, 2005. 102(49): p. 17804-9.

32 Rao, H., S.J. Gillihan, J. Wang, M. Korczykowski, G.M. Sankoorikal, K.A. Kaercher, E.S. Brodkin, J.A. Detre and M.J. Farah, Genetic variation in serotonin transporter alters resting brain function in healthy individuals. Biol Psychiatry, 2007. 62(6): p. 600-6.

Arterial Spin Labeling (*syngo* ASL) Case Reports from Geneva University

Viallon Magalie, Ph.D.; Karl-Olof Lovblad, M.D., Ph.D.

Hopitaux, Universitaire de Genève, Switzerland

Case 1: Pediatric 1

Patient history

15-year-old female patient with known epilepsy.

Image findings / Results

On the T2-weighted images there are multiple bilateral hemispheric cortical and subcortical hyperintensities that are much more visible on the corresponding FLAIR images. On the ASL perfusion maps we have hypoperfusion in these areas.

Discussion

The multiple cortical and subcortical lesions correspond to tubera in a case of Tuberous Sclerosis of Bourneville.

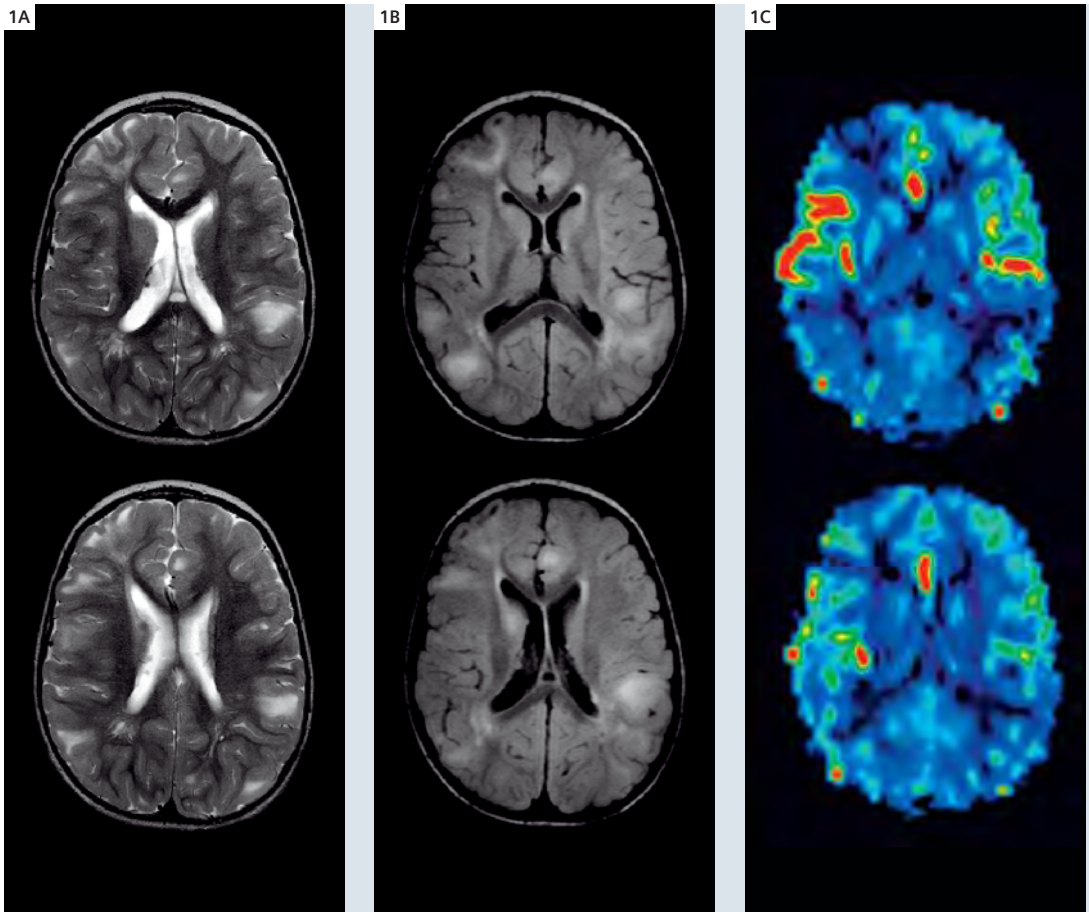

1A T2-weighted axial Turbo Spin Echo (TSE) image. Slice thickness 4 mm, TE/TR 101/4000 ms, BW 170 Hz/px, PAT factor 2, TF 19, FoV 150 x 200 mm, matrix 288 x 512, flip angle 145°.
1B Multiplanar reconstruction (MPR) Flair 3D sagittal 1 mm, TE/TR/TI 411/6000/2100 ms, BW 780 Hz/px, PAT factor 2, TF 266, FoV 234 x 250 mm, matrix 242 x 256, MPR slice thickness 4 mm, 176 slices.
1C Fair-QUIPSII arterial spin labeling sequence: TE/TR 13/5000 ms, BW 2230 Hz/px, matrix 64 x 64, FoV 220 mm, FatSat, slice thickness 6 mm, 14 slices, TI1 700 ms, TI2 1800 ms, T1 1496.5 ms, Partial Fourier 6/8, Lambda 0.9 mL/g, inversion efficiency 95%, flow compensation with flow limit 50 cm/sec, inferior Sat. Thk 100 mm, inferior sat gap 0 mm.

Case 2: Pediatric 2

Patient history

5-months-old* female with intractable epilepsy with 15 episodes per day.

*The safety of imaging infants under two years old has not been established.

Image findings / Results

Polymicrogyria of the left hemisphere on the T2-weighted images. On the ASL perfusion maps there is hypoperfusion in the left occipital lobe, which was also seen on FDG-PET (FluoroDeoxyGlucose-Positron Emission Tomography).

Discussion

Left-sided Hemimegalencephaly with polymicrogyria. The ASL data confirm the PET data which shows ictal hyperperfusion in the left occipital lobe.

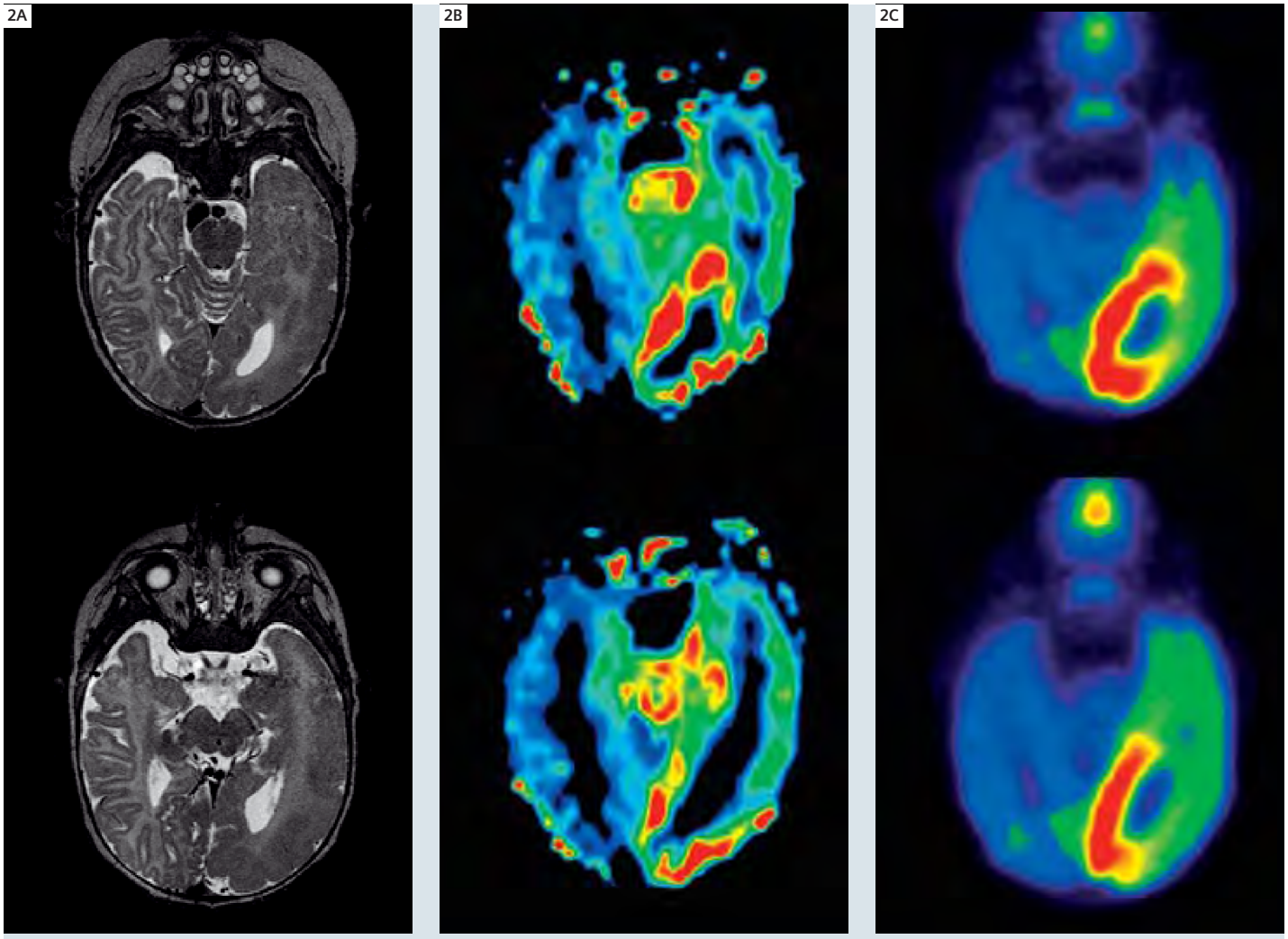

2A T2-weighted axial Turbo Spin Echo (TSE) image, slice thickness mm, TE/TR 101/4000 ms, BW 170 Hz/px, PAT factor 2, TF 19, FoV 150 x 200 mm, matrix 288 x 512, flip angle 145°. **2B** Fair-QUIPSII arterial spin labeling sequence: TE/TR 13/5000 ms, BW 2230 Hz/px, matrix 64 x 64, FoV 220 mm, FatSat, slice thickness 6 mm, 14 slices, TI1 700 ms, TI2 1800 ms, T1 1496.5, Partial Fourier 6/8, Lambda 0.9 mL/g, inversion efficiency 95%, flow compensation with flow limit 50 cm/sec, inferior Sat. Thk 100 mm, inferior sat gap 0 mm. **2C** F18-FDG PET-CT image with attenuation correction from CT data (Siemens Biograph Sensation 16), 80 MBq, 30 min post injection. These images show glucose metabolization which is linked to perfusion even though not being directly an image of CBF.

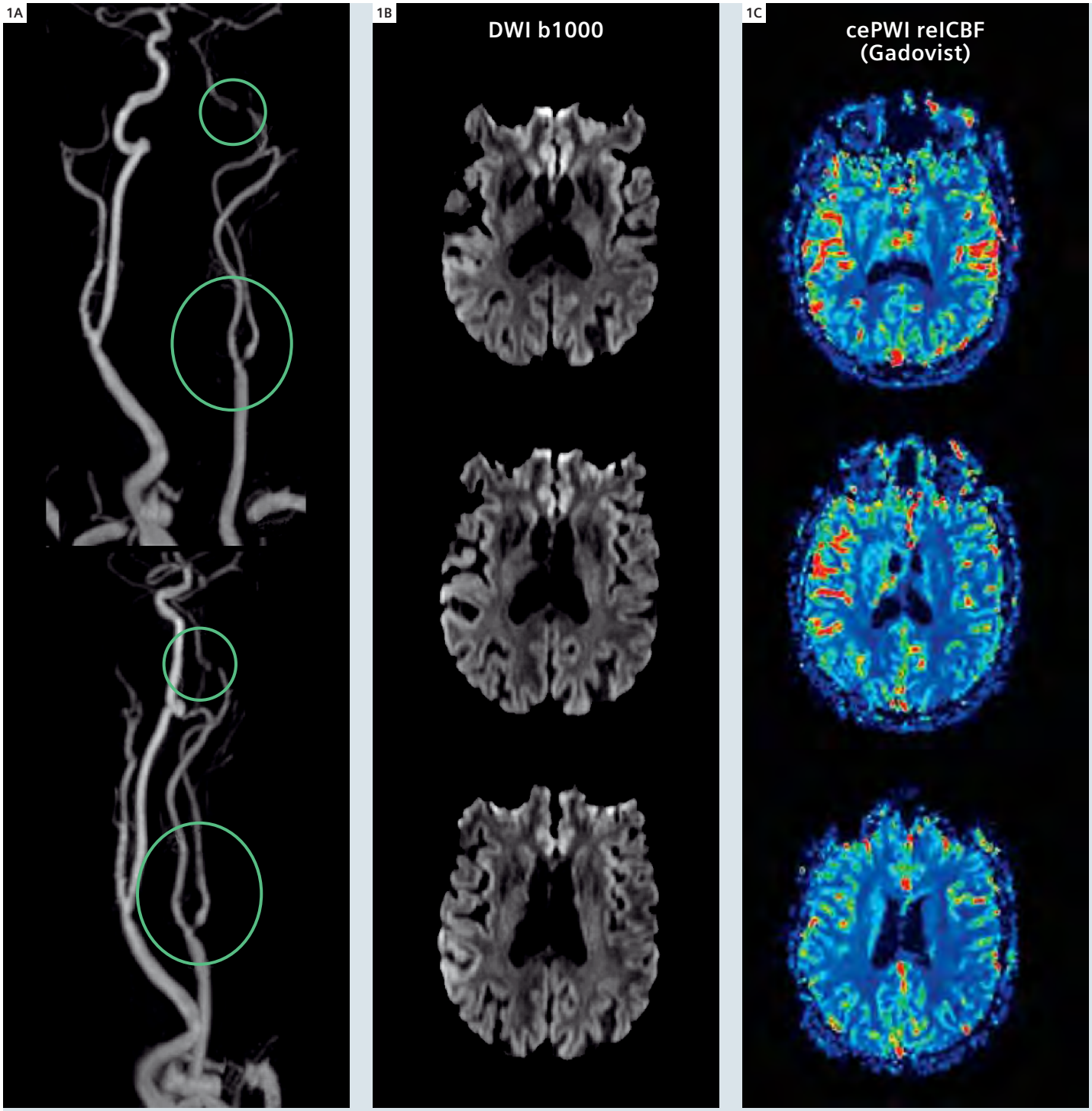

1A Contrast enhanced MR Angiography (ce-MRA): angiogram obtained from Flash3d-ce, voxel 0.8 x 0.8 x 0.8 mm, PAT factor 2, FoV= 263 x 300 mm, matrix 314 x 512, BW 650 Hz/px, flip angle 25°, 88 slices, centric reordering.

1B Diffusion-weighted imaging (DWI) b=1000, slice thickness 4 mm, TE/TR 92/5300 ms, BW 1240 Hz/px, PAT factor 2, FoV 208 x 230 mm, codage AP, matrix 157 x 192, flip angle 90°, 4 averages.

1C Contrast enhanced perfusion-weighed imaging (cePWI)*, relative cerebral blood flow (relCBF)*: relCBF parametric map calculated using *syngo* MR perfusion*, slice thickness 4 mm, TE/TR 92/4000 ms, BW 1370 Hz/px, PAT factor 2, FoV 200 x 200 mm, matrix 128 x 128, flip angle 90°.